Термодинамічним моделюванням із використанням комп'ютерної програми «Thermo-Calc Software» проаналізовано характер формування рівноважного фазового стану при кристалізації наплавлювальних матеріалів У30Х25Н3С3 та 500Х40Н40С2РЦ. Із побудовою діаграм стану встановлено послідовність перетворень, визначено фазовий склад та молярні долі фаз в сплавах в залежності від температури

Ключові слова: наплавлювальні матеріали, термодинамічне моделювання, рівноважна кристалізація, карбіди хрому, карбідна евтектика, аустеніт

Термодинамическим моделированием с использованием компьютерной программы «Thermo-Calc Software» проанализирован характер формирования равновесного фазового состояния при кристаллизации наплавочних материалов У30Х25Н3С3 и 500Х40Н40С2РЦ. С построением диаграмм состояния установлена последовательность превращений, определены фазовый состав и молярные доли фаз в сплавах в зависимости от температуры

Ключевые слова: наплавочные материалы, термодинамическое моделирование, равновесная кристаллизация, карбиды хрома, карбидная эвтектика, аустенит

UDC 621.791.92.042
DOI: 10.15587/1729-4061.2018.124129

SIMULATION OF STRUCTURE FORMATION IN THE Fe–C–Cr–Ni–Si SURFACING MATERIALS

B. Efremenko
Postgraduate student
Department of theory of metallurgical processes and foundry*
E-mail: bodyaefr@gmail.com
A. Belik
PhD, Associate Professor
Department of metallurgy and technology of welding*
E-mail: alexbelick@yandex.ua
Yu. Chabak
PhD, Senior Lecturer
Department of Physics*
E-mail: julia.chabak25@gmail.com
H. Halfa
PhD, Associate Professor
Department of Steel Technology
Central Metallurgical Research and Development Institute
Elfelezat str., 1, Eltebbin, Helwan, Cairo 12422, Egypt
E-mail: hossamhalfa@gmail.com
*Pryazovskyi State Technical University
Universytets'ka str., 7, Mariupol, Ukraine, 87555

1. Introduction

The application of protective coatings using electric arc surfacing is one of the most widely used technologies for renovation and surface strengthening of machine parts and various equipment in the mining-metallurgical, engineering, energy, and other branches of industry. Among the great variety of materials that are used for this purpose, a wide scope of applications characterizes high-carbon compositions based on Fe–C–Cr–Ni–Si-based. Such materials include powder tapes PL AN–101 and PL AN–111 [1]. When surfacing with these tapes, a surfaced metal is obtained, which is denoted as 300Cr25Ni3Si3 ("Sormite–1") and 500Cr40Ni40Si2BZr, respectively [2]. PL AN–101 and PL AN–111 are used for the surfacing of parts of agglomeration and blast-furnace equipment: the contact zones of cones and bowls, the contact surfaces of dishes and valves of bulk devices, bunkers, conveyors of agglomeration machines, etc. Such parts operate under conditions of heavy wear at elevated temperatures [3].

Taking into consideration significant economic losses incurred during downtime of such equipment related to the replacement of worn parts, the quality of surfacing materials should meet enhanced requirements.

2. Literature review and problem statement

By the type of structure, alloys 300Cr25Ni3Si3 and 500Cr40Ni40Si2BZr belong to a group of high-chromium white cast irons known for their high tribological properties [4]. These properties are related to the presence in the microstructure of carbides, borides, carbo-borides, distributed in a metal matrix, which can consist of austenite, ferrite, pearlite, martensite in different combinations and proportions [5]. Paper [6] shows that the highest level of wear resistance of cast irons is reached in the presence of matrix with a structure of metastable austenite. To increase wear resistance, cast irons are additionally alloyed with strong carbide-forming elements, such as Ti, V, Nb, Mo [7], and the rate of crystallization is also increased [8]. Improving the properties of cast iron products is reached by using a heat treatment that includes both the techniques of volume hardening and the technologies of surface modification by the sources of concentrated energy [9].

The main role in high-chromium surfacing compositions belongs to chromium, which provides both high durability and the necessary level of resistance against high-temperature and electrochemical corrosion [10]. Authors of work [11] noted the high level of wear resistance of high-chromium

alloys during tests in liquid corrosion-active environments, particularly in aqueous solutions of sulfuric acid. Article [12] reported that the cast iron with 15 % Cr has an improved resistance against high-temperature corrosion at temperatures up to 1,000 °C inclusive.

The behavior of surfacing coatings under actual industrial conditions is determined by the microstructure and chemical composition of phase components, that is, by factors that should be considered when choosing surfacing materials for specific operating conditions. Based on data from paper [13], chemical composition of the metal obtained by surfacing using the powder tapes PL AN–101 and PL AN–111 enables the formation of structure, resistant to abrasive, gas-abrasive, erosive wear under ambient and elevated temperatures. This is due to the high corrosion- and heat resistance of the metal matrix combined with the strengthening carbide phases. Since the tribological properties of the surfacing metal are determined first of all by its microstructure, the prediction of micro-structural state in the surfacing coatings becomes very important [14]. This is also emphasized by authors of article [15] who studied the relationship "wear resistance – hardness – microstructure" relative to Fe–Cr–C and Fe–Cr–C–B surfacing materials.

There are known papers that deal with powder tapes PL AN–101 and PL AN–111 [1–3, 13], mainly focusing on the technological peculiarities of surfacing and the level of welding quality for the surfaces coatings obtained. In contrast, the character of structure formation in the coatings obtained using the powder tapes PL AN–101 and PL AN–111 remains insufficiently studied, and therefore requires more detailed research. Such a study could be conducted employing a thermodynamic simulation [16]. Simulation results typically reflect a thermodynamically-stable state of the system, which is formed during crystallization of the alloy under equilibrium conditions, that is, at a very low cooling rate. Real conditions of structure formation in a coating that is applied (by surfacing, spraying, etc.) are characterized by the instability of processes, which may lead to consequences that differ from the results of simulation. However, it yields information about the character of transformations and structural changes that are fundamentally possible for the alloy of a given chemical composition. This makes it possible to assess the impact of technological parameters of the process of application on the resulting microstructure of the coating, which is important given the possibility to control the quality of metal through the optimization of technology.

3. The aim and objectives of the study

The aim of present work is to analyze patterns in the formation of a microstructure and the phase state of the alloys 300Cr25Ni3Si3 and 500Cr40Ni40Si2BZr at crystallization. This would make it possible to predict behavior of the alloys under actual conditions of wear and to choose appropriate variants for their application in practice.

To accomplish the aim, the following tasks have been set:

– to determine the character of phase transformations and the dynamics of change in the molar fraction of phases during crystallization of alloys under equilibrium conditions;

– to establish thermodynamic characteristics and the equilibrium chemical composition of phase components.

4. Materials and procedure for thermodynamic simulation of alloy crystallization

We have chosen, as the material to be examined, alloys of the alloying system Fe–C–Cr–Ni–Si–Mn whose chemical compositions are given in Table 1.

Table 1

Chemical composition of the alloys 300Cr25Ni3Si3 and 500Cr40Ni40Si2BZr

Tape (alloy)	Content, % by weight:							
	C	Cr	Ni	Si	Mn	B	Zr	Fe
PL AN-101 (300Cr25Ni3Si3)	3.0	25.0	3.0	3.0	2.0	–	–	balance
PL AN-111 (500Cr40Ni40Si2BZr)	5.0	40.0	40.0	2.0	1.0	0.1	0.5	balance

The character of structure formation during crystallization was studied by thermodynamic simulation employing the "Thermo-Calc Software" based on the method for calculating the equilibrium phase diagrams CALPHAD [17]. This software makes it possible to build and analyze state diagrams of multicomponent alloys and to determine the thermodynamic characteristics of phase components of the structure.

Calculations of thermodynamic characteristics of the components and the phase chemical composition using the "Thermo-Calc Software" were conducted at the following initial parameters: temperature is 1,000 K, pressure is atmospheric (10^5 Pa), the degree of freedom is 0, the content of chemical elements in weight percentage is in accordance with Table 1. Atmospheric pressure was chosen relative to the normal conditions of alloy crystallization; the temperature of 1,000 K (727 °C) corresponds to the completion of all the transformations and the formation of the resulting phase state in alloys.

5. Results of study into the structure formation in alloys

5. 1. Alloy 300Cr25Ni3Si3

Fig. 1 shows a phase diagram of the system Fe – 25 % Cr – 3 % Ni– 3 % Si – 2 % Mn – C, which includes the alloy 300Cr25Ni2Si3 ("Sormite–1"). Positions of this alloy in the diagram are marked with a dotted line. It follows from the Figure that the alloy 300Cr25Ni3Si3 refers to the hypereutectic alloys. Its crystallization starts at a temperature below 1,355 °C (liquidus temperature) from the formation of primary carbides M_7C_3 with a hexagonal lattice of the spatial group *Pnma*. In the temperature range of 1,255–1,236 °C, there the eutectic reaction "L→Austenite (FCC_A1)+M_7C_3" occurs. At temperatures in the range of 1,236–830 °C, the alloy is in a two-phase state, comprising austenite and carbides M_7C_3 (primary and eutectic). At a temperature below 830 °C, the alloy is in a three-phase state, that is, consists of austenite, ferrite (BCC_A2) and carbides M_7C_3.

Change in the phase composition of the alloy 300Cr25Ni3Si3 at crystallization is illustrated by Fig. 2. At the time of start of the eutectic transformation, the alloy consists of 80 mol. % liquid and 20 mol. % primary carbides M_7C_3; and upon its completion – of 64 mol. % austenite and 36 mol. % carbides M_7C_3 (primary and eutectic). In the range of 1,236–830 °C, molar fraction of carbides gradually

rises to 39 mol. % with a corresponding decrease in the fraction of austenite. Starting at 830 °C, ferrite appears in the structure; in the range of 830–600 °C, there is a gradual increase in the fraction of ferrite with a decrease in the fraction of austenite. At 600 °C, the alloy 300Cr25Ni2Si3 consists of 54 mol. % ferrite, 41 mol. % M_7C_3, and 5 mol. % austenite.

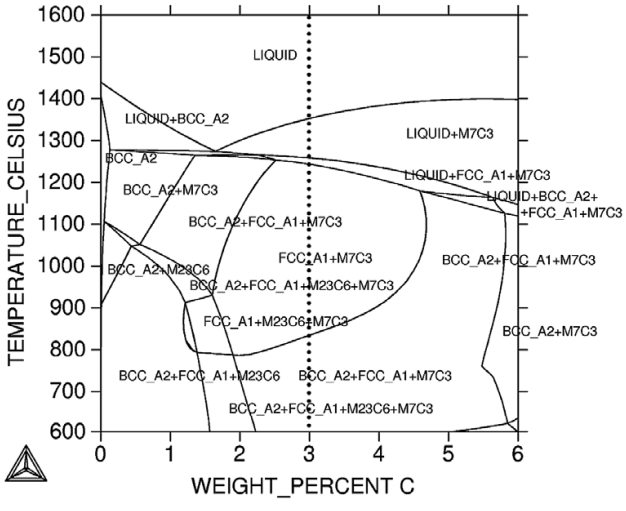

Fig. 1. Phase diagram of the system Fe – 25 % Cr – 3% Ni – 3 % Si – 2 % Mn – C

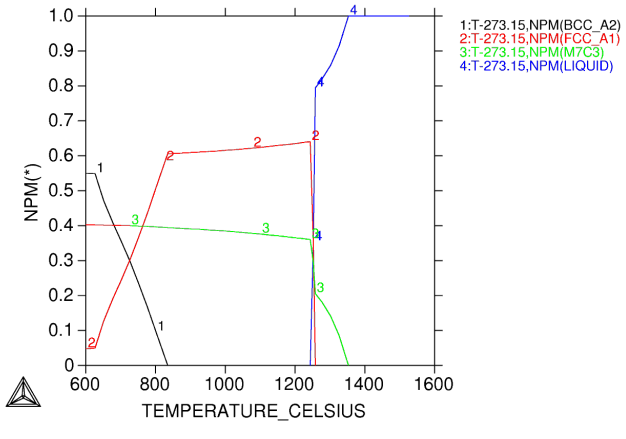

Fig. 2. Change in phase composition (in molar parts) of the alloy 300Cr25Ni3Si3 dependent on temperature

Thermodynamic characteristics of components and the phase chemical composition, calculated for 1,000 K (727 °C) and a pressure of 10^5 Pa, are given in Tables 2, 3. Under these conditions, we obtained the following data for the alloy 300Cr25Ni3Si3: molar mass is 48.29 g/mol.; enthalpy (ΔH_{1000}^{o}) is 1.40×10^4 J/mol.; Gibbs energy (ΔG_{1000}^{o}) is (-5.18×10^4) J/mol. According to data from Table 3, the alloy is characterized by a significant intraphase redistribution of chemical elements. At 1,000 K, the main mass of austenite-stabilizing elements (manganese and nickel) is concentrated in austenite, while ferrite-forming silicon is concentrated mainly in ferrite. The concentration of chromium in approximately the same in both matrix phases, while its larger part (70 % by weight) is in carbides. Carbide M_7C_3 contains chromium, iron, manganese, and nickel. Austenite has low carbon content, which is associated with the solid-phase reaction of precipitation of carbides M_7C_3 from it at temperatures below the interval of eutectic transformation.

Table 2

Thermodynamic characteristics of components in the alloy 300Cr25Ni3Si3 (at 1,000 K and 10^5 Pa)

Components	Molar fraction	Activity	Potential, J/mol.
C	0.121	2.80×10^{-2}	-2.97×10^4
Cr	0.232	1.12×10^{-3}	-5.65×10^4
Fe	0.553	4.39×10^{-3}	-4.51×10^4
Mn	0.018	2.18×10^{-5}	-8.92×10^4
Ni	0.025	5.11×10^{-4}	-6.30×10^4
Si	0.052	8.29×10^{-8}	-1.35×10^5

Table 3

Equilibrium phase composition of the alloy 300Cr25Ni3Si3 (at 1,000 K and 10^5 Pa)

Phase	Content of elements, % by weight:					
	C	Cr	Mn	Ni	Si	Fe
BCC_A2#1 (ferrite)	0.001	1.88	1.16	1.92	5.22	89.82
FCC_A1#1 (austenite)	0.06	2.42	3.28	6.76	3.83	83.65
M7C3#1 (carbide M_7C_3)	8.88	70.18	1.54	0.28	0.00	19.12

According to the results of thermodynamic simulation, the equilibrium structure of the alloy 300Cr25Ni3Si3 consists of primary carbides M_7C_3 and carbide eutectic "Matrix+ M_7C_3", where matrix is a mixture of ferrite and austenite.

5. 2. Alloy 500Cr40Ni40Si2BZr

A phase diagram of the system Fe–40 % Cr–40 % Ni–2 % Si–1 % Mn–C is shown in Fig. 3; phase composition of the alloy 500Cr40Ni40Si2BZr, depending on temperature, is in Fig. 4.

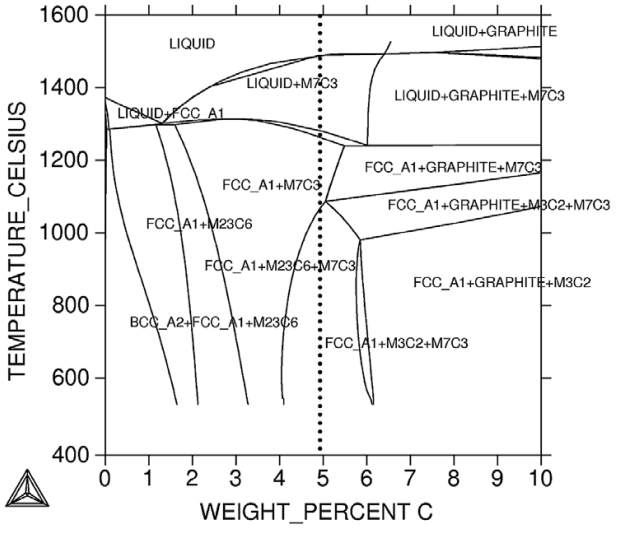

Fig. 3. Phase diagram of the system Fe – 40 % Cr – 40 % Ni – 2 % Si – 1 % Mn – C

The diagram (Fig. 3) was built disregarding zirconium due to the absence of this element in the computer database TCFE7, which was employed during simulation. Since zirconium is a strong carbide-forming element, it is almost entirely associated with carbon to form cubic carbide ZrC_x

that is crystallized directly from liquid at high temperatures to form chromium carbides [18]. The ratio of zirconium to carbon atoms in a molecule of carbide ZrC_x is 7.6:1. Given this ratio, when 0.5 % zirconium is introduced to the alloy, it will bind 0.06 % of carbon. Then crystallization of the alloy 500Cr40Ni40Si2BZr will actually proceed in accordance with the content of carbon in the liquid equal to 4.94 % (position of this alloy is marked with a dotted line in Fig. 3). Thus, the resulting diagram can be applied to predict the structure in the alloy 500Cr40Ni40Si2BZr.

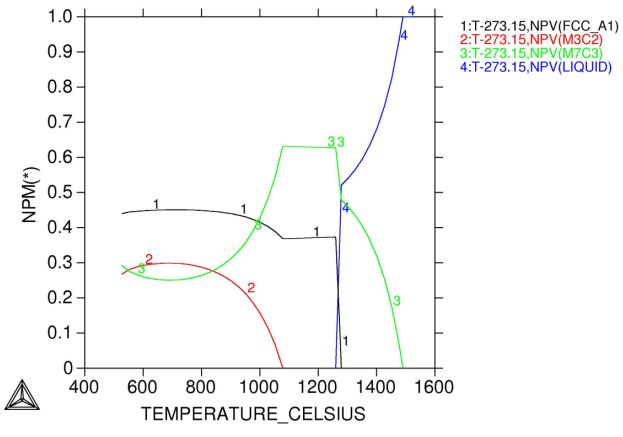

Fig. 4. Change in phase composition (in molar parts) of the alloy 500Cr40Ni40Si2BZr, dependent on temperature

Similar to 300Cr25Ni3Si3, the alloy 500Cr40Ni40Si2BZr refers to hypereutectic alloys. Its crystallization starts at 1,485 °C with the precipitation of primary carbides M_7C_3 from liquid (48 mol % M_7C_3 is maximally precipitated). The rest of the liquid crystallizes in line with the eutectic reaction of "L→Austenite (FCC_A1)+M_7C_3" in the temperature range of 1,285–1,263 °C; upon completion of the reaction, the alloy contains 62.5 mol. % carbides M_7C_3 and 37.5 mol. % austenite.

At temperatures below 1,081 °C, the alloy would contain carbide M_3C_2 with a rhombic lattice of the spatial group *Pnma*. The alloy undergoes carbide transformations: first, in the range of 1,081–690 °C, there the reaction "M_7C_3→Austenite + M_3C_2" occurs. As a result, the amount of carbide M_7C_3 reduces to 25 mol. %, while the amount of austenite and rhombic carbide M_3C_2 rises to 45 mol. % and 30 mol. %, respectively. Next, in the temperature range of 690–500 °C, there is a reverse transformation "Austenite+M_3C_2→M_7C_3". It leads to an increase in the mole fraction of carbide M_7C_3 to 29.5 mol. % with a corresponding decrease in the fraction of austenite to 44 mol. % and carbide M_3C_2 – to 26.5 mol. %.

Thermodynamic characteristics of components and the chemical composition of phases (for 1,000 K and atmospheric pressure) are given in Tables 4, 5. We obtained for the alloy 500Cr40Ni40Si2BZr: molar mass is 48.47 g/mol.; enthalpy (ΔH_{1000}^{o}) is 1.48×10^4 J/mol.; Gibbs energy (ΔG_{1000}^{o}) is (-1.90×10^4) J/mol.

It follows from Table 5 that nickel and silicon are almost entirely concentrated in austenite, while carbon and chromium are in carbides M_7C_3 and M_3C_2. A comparison of Tables 3, 5 shows that carbides in the alloy 500Cr40Ni40Si2BZr contain significantly more chromium (by 16–16.5 %) and significantly less iron (by 13–19 %) than in the alloy 300Cr25Ni3Si3. Nickel is instead almost entirely missing in carbides in the alloy 500Cr40Ni40Si2BZr in contrast to 300Cr25Ni3Si3.

Table 4

Thermodynamic characteristics of components in the alloy 500Cr40Ni40Si2BZr (at 1,000 K and 10^5 Pa)

Components	Molar share	Activity	Potential, J/mol.
C	0.121	3.28×10^{-3}	-4.76×10^4
Cr	0.372	5.33×10^{-1}	-5.22×10^3
Fe	0.119	1.76×10^{-1}	-4.44×10^4
Mn	0.00882	8.32×10^{-4}	-5.90×10^4
Ni	0.0330	2.91×10^{-1}	-1.03×10^4
Si	0.0345	4.99×10^{-7}	-1.21×10^5

Table 5

Equilibrium phase chemical composition of the alloy 500Cr40Ni40Si2BZr (at 1,000 K and 10^5 Pa)

Phase	Content of elements, % by weight:					
	C	Cr	Mn	Ni	Si	Fe
FCC_A1#1 (austenite)	0.0001	13.18	1.75	60.45	2.75	21.96
M7C3#1 (carbide M_7C_3)	8.92	86.19	1.53	0.007	0.00	3.36
M3C2#1 (carbideM_3C_2)	13.33	86.67	0.00	0.00	0.00	0.00

Thus, according to the results of simulation in a thermodynamically-steady state, the alloy 500Cr40Ni40Si2BZr has a microstructure that consists of austenite, hexagonal carbide M_7C_3 and rhombic carbide M_3C_2.

6. Discussion of results of thermodynamic simulation

The results obtained showed that at low cooling, a hypereutectic structure forms in the alloys 300Cr25Ni3Si3 and 500Cr40Ni40Si2BZr with a large quantity of carbide phases. In this case, molar fraction of carbides in the alloy 500Cr40Ni40Si2BZr is higher than that in 300Cr25Ni3Si3 (56 mol. % against 41 mol. %). The difference in the amount of carbides can be differently reflected on the ratio of abrasive/erosive wear resistance of alloys depending on the dynamics of contact between an abrasive particle and the surface. Under conditions of the impact contact, at the angles of attack from 30 to 60 degrees, there is the possibility of cracking and chipping of primary carbides, which will lead to a reduced level of wear resistance for 500Cr40Ni40Si2BZr. These processes can be amplified at the expense of residual stresses, which are a characteristic feature of welding and surfacing [19]. In a contact at the angles close to the tangential or normal directions, the presence of a great amount of carbides can provide this alloy with improved wear resistance.

Significant differences in the chemical composition of carbides in the analyzed alloys may cause a difference in the microhardness of carbide phases in favor of the alloy 500Cr40Ni40Si2BZr. This may be due to the higher content of chromium with a corresponding increase in the covalent component in the intra-atomic bonds [20].

The high concentration of nickel (40 %) in the alloy 500Cr40Ni40Si2BZr ensures the formation of an austenitic structure of the metal matrix in it, while the lack of nickel

in the alloy 300Cr25Ni3Si3 leads to the formation of a two-phase ($\alpha+\gamma$) state of the matrix.

It follows from Fig. 3 that the alloy 500Cr40Ni40Si2BZr under thermodynamically equilibrium conditions misses the graphite phase. However, even at 5.5 %, the alloy contains graphite, which is formed in alloys with 5.5–6.0 % of C at 1,240 °C in line with the eutectic reaction "L→Austenite (FCC_A1)+M_7C_3+Graphite". At carbon content above 6.0 % graphite begins to crystallize from the liquid at a temperature above 1,500 °C even before the formation of primary carbides M_7C_3. According to the results of simulation, the amount of graphite at 5.5–6.0 % of C can reach 3–4 mol. %. Thus, the alloy 500Cr40Ni40Si2BZr is close enough to a concentration interval of the existence of graphite phase, which is important concerning the negative impact of the latter on the abrasive (erosive) wear resistance of alloys. At slight variations in the composition of a powder tape, or as a result of insufficient mixing of elements during crystallization of the surface coating, it may be subject to the emergence of carbon enriched zones, where conditions for the formation of graphite would be created.

A study of structure formation by thermodynamic simulation has certain limitations. They arise from the conditions of achieving a thermodynamically-stable state of the system, which implies the low rate of crystallization. This leads to possible shortcomings in present research, related to the possibility of incomplete conformity of simulation results with the actual condition of the microstructure, which forms at very high cooling rates, characteristic of electric arc application of coatings.

The benefit of present study includes the obtaining of theoretically substantiated data on the type of phases, their stoichiometric chemical composition and volumetric ratio, which reflect the nature of interatomic interaction in the multicomponent alloys 300Cr25Ni3Si3 and 500Cr40Ni40Si2BZr. This is especially true for the latter alloy. It differs from most of the Fe–Cr–C surfacing materials by the replacement of a significant amount of iron with nickel, and therefore refers to a different alloying system (Ni–Cr–C), which has been explored in much lesser extent.

The results obtained could be useful in practice when determining the feasibility of application of surfacing materials under actual operating conditions, as well as when controlling the structural state of a coating by optimizing technological parameters of its application.

Further development of present work could involve a research into a real microstructure and phase state of the alloys 300Cr25Ni3Si3 and 500Cr40Ni40Si2BZr, surfaced with the powder tapes PL AN-101 and PL AN-111, respectively. This would make it possible to estimate the degree of match between actual (non-stationary) and thermodynamically-equilibrium conditions of crystallization in order to take it into consideration in future when modeling the processes of structure formation in alloys with different chemical composition. In this case, one should pay attention to the need for a correct choice of databases at simulation, which would make it possible to obtain adequate results for the alloys of a particular alloying system.

7. Conclusions

1. By using thermodynamic simulation employing the "Thermo-Calc Software", we investigated the character of crystallization of the alloys 300Cr25Ni3Si3 and 500Cr40Ni40Si2BZr under equilibrium conditions. It was established that their crystallization starts with the formation of primary carbides M_7C_3, followed by the eutectic reaction "Liquid→Austenite+M_7C_3". Solid-phase structural transformations also occur in the alloys, specifically: in 300Cr25Ni3Si3 – transformation of austenite into ferrite (below 830 °C), in 500Cr40Ni40Si2BZr – carbide transformation $M_7C_3 \leftrightarrow M_3C_2$ (below 1,081 °C).

2. We have defined a thermodynamically-stable phase state of the alloys, which at temperatures below 700 °C is represented by the following set of phases: in the alloy 300Cr25Ni3Si3 – austenite, ferrite, carbide M_7C_3; in the alloy 500Cr40Ni40Si2BZr – austenite, carbide M_7C_3, carbide M_3C_2. We calculated thermodynamic characteristics and obtained stoichiometric chemical composition and a molar fraction of the specified phases in the structure of each of the alloys.

References

1. Voronchuk A. P. Poroshkovye lenty dlya iznosostoykoy naplavki // Avtomaticheskaya svarka. 2014. Issue 6-7. P. 75–78.
2. Chigarev V. V., Belik A. G. Flux-cored strips for surfacing // Welding International. 2012. Vol. 26, Issue 12. P. 975–979. doi: 10.1080/09507116.2012.694643
3. Zhudra A. P., Voronchuk A. P. Naplavochnye poroshkovye lenty // Avtomaticheskaya svarka. 2012. Issue 1. P. 39–44.
4. High Wear Resistance of White Cast Iron Treated by Novel Process: Principle and Mechanism / Jia X., Zuo X., Liu Y., Chen N., Rong Y. // Metallurgical and Materials Transactions A. 2015. Vol. 46, Issue 12. P. 5514–5525. doi: 10.1007/s11661-015-3137-4
5. Abrasive wear of V–Nb–Ti alloyed high-chromium white irons / Bedolla-Jacuinde A., Guerra F. V., Mejía I., Zuno-Silva J., Rainforth M. // Wear. 2015. Vol. 332–333. P. 1006–1011. doi: 10.1016/j.wear.2015.01.049
6. Abrasive resistance of metastable V–Cr–Mn–Ni spheroidal carbide cast irons using the factorial design method / Efremenko V. G., Shimizu K., Cheiliakh A. P., Pastukhova T. V., Chabak Y. G., Kusumoto K. // International Journal of Minerals, Metallurgy, and Materials. 2016. Vol. 23, Issue 6. P. 645–657. doi: 10.1007/s12613-016-1277-1
7. Effect of Ti-V-Nb-Mo Addition on Microstructure of High Chromium Cast Iron / Youping M., Xiulan L., Yugao L., Shuyi Z., Xiaoming D. // China Foundry. 2012. Vol. 9, Issue 2. P. 148–153.
8. Pulsed plasma deposition of Fe-C-Cr-W coating on high-Cr-cast iron: Effect of layered morphology and heat treatment on the microstructure and hardness / Efremenko V. G., Chabak Y. G., Lekatou A., Karantzalis A. E., Shimizu K., Fedun V. I. et. al. // Surface and Coatings Technology. 2016. Vol. 304. P. 293–305. doi: 10.1016/j.surfcoat.2016.07.016

9. Effect of bulk heat treatment and plasma surface hardening on the microstructure and erosion wear resistance of complex-alloyed cast irons with spheroidal vanadium carbides / Efremenko V. G., Shimizu K., Pastukhova T. V., Chabak Y. G., Kusumoto K., Efremenko A. V. // Journal of Friction and Wear. 2017. Vol. 38, Issue 1. P. 58–64. doi: 10.3103/s1068366617010056
10. Microstructure of high (45 wt. %) chromium cast irons and their resistances to wear and corrosion / Tang X. H., Chung R., Pang C. J., Li D. Y., Hinckley B., Dolman K. // Wear. 2011. Vol. 271, Issue 9-10. P. 1426–1431. doi: 10.1016/j.wear.2010.11.047
11. Microstructure And Erosion-Corrosion Behaviour Of As-Cast High Chromium White Irons Containing Molybdenum In Aqueous Sulfuric-Acid Slurry / Imurai S., Thanachayanont C., Pearce J. T. H., Chairuangsri T. // Archives of Metallurgy and Materials. 2015. Vol. 60, Issue 2. P. 919–923. doi: 10.1515/amm-2015-0230
12. High-Temperature Oxidation and Decarburization of 14.55 wt pct Cr-Cast Iron in Dry Air Atmosphere / Efremenko V. G., Chabak Y. G., Lekatou A., Karantzalis A. E., Efremenko A. V. // Metallurgical and Materials Transactions A. 2016. Vol. 47, Issue 4. P. 1529–1543. doi: 10.1007/s11661-016-3336-7
13. Malinov V. L., Chigarev V. V., Vorob'ev V. V. Novye poroshkovye lenty dlya naplavki detaley, rabotayushchih v usloviyah abrazivnogo i gazoabrazivnogo vozdeystviya // Zakhyst metalurhiynykh mashyn vid polomok. 2012. Issue 14. P. 252–258.
14. Microstructure and wear characteristics of high-carbon Cr-based alloy claddings formed by gas tungsten arc welding (GTAW) / Lin C.-M., Chang C.-M., Chen J.-H., Hsieh C.-C., Wu W. // Surface and Coatings Technology. 2010. Vol. 205, Issue 7. P. 2590–2596. doi: 10.1016/j.surfcoat.2010.10.004
15. Yüksel N., Şahin S. Wear behavior–hardness–microstructure relation of Fe–Cr–C and Fe–Cr–C–B based hardfacing alloys // Materials & Design. 2014. Vol. 58. P. 491–498. doi: 10.1016/j.matdes.2014.02.032
16. Ilinykh N., Krivorogova A. Thermodynamic modeling of fluxing alloys of Ni-C-Cr-Si-B system // The European Physical Journal Special Topics. 2017. Vol. 226, Issue 5. P. 1115–1121. doi: 10.1140/epjst/e2016-60240-0
17. Phase Diagram Calculation and Analyze on Cast High-Boron High-Speed Steel / Yang Y., Fu H., Lei Y., Wang K., Zhu L., Jiang L. // Journal of Materials Engineering and Performance. 2015. Vol. 25, Issue 2. P. 409–420. doi: 10.1007/s11665-015-1847-9
18. Tugoplavkie karbidy / G. V. Samsonov (Ed.). Kyiv: Naukova dumka, 1970. 276 p.
19. Fatigue crack growth resistance of welded joints simulating the weld-repaired railway wheels metal / Ostash O. P., Kulyk V. V., Poznyakov V. D., Haivorons'kyi O. A., Markashova L. I., Vira V. V. et. al. // Archives of Materials Science and Engineering. 2017. Vol. 2, Issue 86. P. 49–52. doi: 10.5604/01.3001.0010.4885
20. Beneficial Effects of the Core–Shell Structure of Primary Carbides in High-Cr (45 wt%) White Cast Irons on Their Mechanical Behavior and Wear Resistance / Tang X. H., Li L., Hinckley B., Dolman K., Parent L., Li D. Y. // Tribology Letters. 2015. Vol. 58, Issue 3. doi: 10.1007/s11249-015-0522-5